DOI:
10.1021/acsomega.9b04369

Document Version
Peer reviewed version

Identifying the responses from the estrogen receptor expressed MCF7 cells treated in anticancer drugs of different modes of action using live-cell FTIR spectroscopy

Ali Altharawi[a,b], Khondaker Miraz Rahman[a] and Ka Lung Andrew Chan[a]*

[a] Institute of Pharmaceutical Science, School of Cancer studies and Pharmaceutical Sciences, King's College London, SE1 9NH

[b] College of Pharmacy, Prince Sattam Bin Abdulaziz University, Kingdom of Saudi Arabia, Al-Kharj 16278

Abstract

Recently, we have shown that changes in Fourier transform infrared (FTIR) spectra of living MDA-MB-231 cells (a triple negative cell line) upon exposure to anticancer drugs reflect the changes in the cellular compositions that is correlated to the modes of action of drugs. In the present study, we studied an estrogen receptor expressing breast cancer cell line, MCF7, exposed in three anticancer drugs belonging to two well-characterised anticancer classes; selective estrogen receptor modulators (SERMs) and DNA-intercalating agent. Firstly, we evaluated if the spectral changes in cells are according to the modes of action of drugs and the characteristics of the MCF7 cell line in the same way as the MDA-MB-231 cell. Living MCF7 cells were treated in the three drugs at IC50 concentration, and the difference spectra were analysed using principal component analysis (PCA). The results demonstrated a clear separation between tamoxifen/toremifene (SERMs)-treated cells from the doxorubicin (DNA-intercalator)-treated and untreated cells (control). Tamoxifen and toremifene induced similar spectral changes in the cellular compositions of MCF7 cells and lead to the clustering of these two drugs in the same quadrant of the principal component 1 (PC1) versus PC2 score plots. The separation is mostly attributed to their similar modes of actions. However, doxorubicin-treated MCF7 cells highlighted spectral changes that are mainly occurred in bands at 1085, and 1200-1240 cm^{-1}, which could be associated with the DNA-intercalation effects of the drug. Secondly, the pairwise PCA at various individual time points was employed to investigate whether the spectral changes of MCF7 and MDA-MB-231 cells in response to the IC50 of tamoxifen/toremifene and doxorubicin are dependent on the characteristics of the cell lines. The estrogen expressing MCF7 cells demonstrated significant differences in response to the SERMs in comparison to the triple negative MDA-MB-231 cells suggesting different modes of action have taken place in the two tested cell lines. In contrast, the doxorubicin-treated MDA-MB-231 and MCF7 cells shows similar changes in the 1150-950 cm^{-1}, which indicates the DNA intercalation effect of doxorubicin are found in both cell lines. The results have demonstrated that live-cell FTIR analysis is sensitive to the different modes of action from the same drugs on cells with different characteristics.

Keywords: FT-IR; Live cells, PCA, Vibrational spectroscopy, Anticancer agents, Modes of action

Accepted by ACS Omega on 26-Mar-2020.

Introduction

The development of anticancer drugs is a complex, time-consuming and costly process. It takes more than ten years of development and cost approximately $1 billion on average.[1, 2] Despite the excessive efforts intended for inventing new anticancer drugs, the number of new drugs has not yet met the increasing demand. The attrition rate is considerably high, and only 5% of cancer drugs entering clinical trials have successfully reached the marketing approval.[3, 4] As a result, the classical screening approaches (cell-free or cell-based) have been re-evaluated, and progressively new techniques have been developed. Unlike classical approaches, these new techniques provide mechanistic information on the interaction of putative drugs with their targets. Metabolomics (the study of metabolites profile in biological systems such as cells and tissues) is a promising tool that gives a holistic view on the interaction of drugs with cells.[5] Various techniques such as mass spectroscopy, nuclear magnetic resonance have been employed in metabolomics.[6] However, these techniques are laborious, destructive and involve high capital cost equipment. Considering these limitations, it would be interesting to develop a screening approach based on FTIR spectroscopy.

FTIR spectroscopy is a non-destructive and low-cost technique that can provide a holistic view of the chemical composition of biological samples. It is increasingly finding applications in the study of drug-cell interaction and present itself as a feasible technique for drug screening.[7-9] Evidence of the effects of drugs on the cells can be inferred by acquiring the IR spectra of drug-treated cells. Several studies established numerous applications including, but are not limited to, the assessment of the effectiveness of cancer drugs against several types of cancer and distinguishing classes of anticancer drugs based on spectral changes that reflect the mode of actions of drugs.[10-14] For instance, the effects of four structurally-related anticancer cardiotonic steroids on prostate cancer cell line (PC-3) were investigated using FTIR spectroscopy, and the results demonstrated that unique spectral signatures can be observed from the different cellular pathway between the tested compounds.[15] In a similar study, FTIR spectroscopy was employed to investigate the response of PC-3 cells to seven anticancer drugs belongs to three different classes. It was demonstrated that drugs that are known to induce similar effects appeared to cluster closely based on the resemblance of spectral features.[16] Another study employed synchrotron radiation infrared microspectroscopy to distinguish classes of anticancer drugs that are known to have different effects on A2780 ovarian cancer cells. The results demonstrated a clear distinction between drugs from different modes of actions and untreated cells.[17]

The previously mentioned studies were conducted on chemically fixed or dry cells to benefit from the easy handling of the samples and avoid the dominance of water signal in the mid-IR

regions. These studies provided invaluable biochemical information about changes in the cellular compositions in response to treatment; either at a single-cell level or as a population of cells. However, the chemical fixation has been shown to cause various changes of structures within cells, and hence, it may influence the spectral features of cells exposed to anticancer drugs.[18-21] The study of live cells in their aqueous environment using FTIR spectroscopy has been made available using the multi-reflection attenuated total reflection (ATR) sampling method. Although water is a major obstacle in the IR study of live cells,[22] the spectra of live cells can be acquired with a high signal-to-noise ratio (SNR) using the multi-reflection ATR approach.[23, 24] The proposed *in-situ* approach provides two main advantages; it eliminates the artefacts originated from drying and fixing cells and allows continuous monitoring of the response of living cells exposed to anticancer drugs. The latter advantage enables a real-time probing of the changes in the major cellular compositions such as proteins, nucleic acids and phosphorylated compounds. Therefore, it further enhances the predictability of this approach in the study of drug-cell interaction as cellular changes can be tracked at different time points in the same experiment.

We have recently shown that ATR FTIR spectroscopy combined with principal component analysis (PCA) is a powerful technique to distinguish the response of MDA-MB-231 cells, a triple negative cell, based on their different modes of actions. The results have shown that drugs with the same mode of action (tamoxifen and toremifene) were clustered together and well-separated from the other drugs of different modes of action (imatinib and doxorubicin).[25]

In the present work, a different cell line, MCF7, which is known to express oestrogen, progesterone and HER2 receptor (triple positive) is utilised to evaluate if the different mode of actions of the same drug on different cell line can also be distinguished using the live cell FTIR approach. MCF7 and MDA-MB-231 cells are both commonly-used breast cancer cell lines as an *in vitro* model to study breast cancer biology. Both cells used in the National Cancer Institute (NCI60) screening program and in research for the development of anticancer drugs as well as in understanding drug resistance.[26] Studies have demonstrated different biochemical pathways for the response of MCF7 and MDA-MB-231 cells to the selective oestrogen receptor modulators (SERMs) such as tamoxifen and toremifene. The cytotoxicity of tamoxifen against the triple negative breast cancer cells (e.g. MDA-MB-231) has shown to be mediated through an oestrogen-independent pathway.[27] However, tamoxifen induces cytotoxicity in MCF7 cells mainly through an oestrogen-dependent pathway.[28] To our knowledge, this is the first study utilised FTIR spectroscopy to compare two breast cancer cells (having different expression level of oestrogen receptor) in response to the same drugs and investigate if the induced spectral changes correlate with the different modes of actions.

Furthermore, the response of MCF7 cells to doxorubicin (DNA-intercalating agent) aimed to investigate if the spectral changes of a specific mode of action are similar for both cell lines.

Results and Discussion

The attachment and growth of MCF7 cells on the ZnS ATR element in the culture medium (i.e. L-15 medium) was first examined for the time of the experiment (in total, approximately 72 h from seeding the cells). The cells were seeded at high density (~200,000 cells/cm^2) to ensure a monolayer of cells is formed. **Figure 1A** shows the typical FTIR spectra of MCF7 cells with the absorbance of amide II (1545 cm^{-1}) reproducibly reaching a plateau of ~0.22 a.u. after 72 h from seeding. The growth of the absorbance of amide II slowed after 24 h of seeding suggesting that the cell has reached the plateau phase. This enables the detection of the subtle changes in cellular compositions after the addition of the drugs at the 24th hour. The averaged spectra of the 24th and 48th hour after seeding the cells from four repeated experiments, each from a separate culture, are presented in Figure 1B and C. The high reproducibility of the experiment was indicated by the small standard deviation shown.

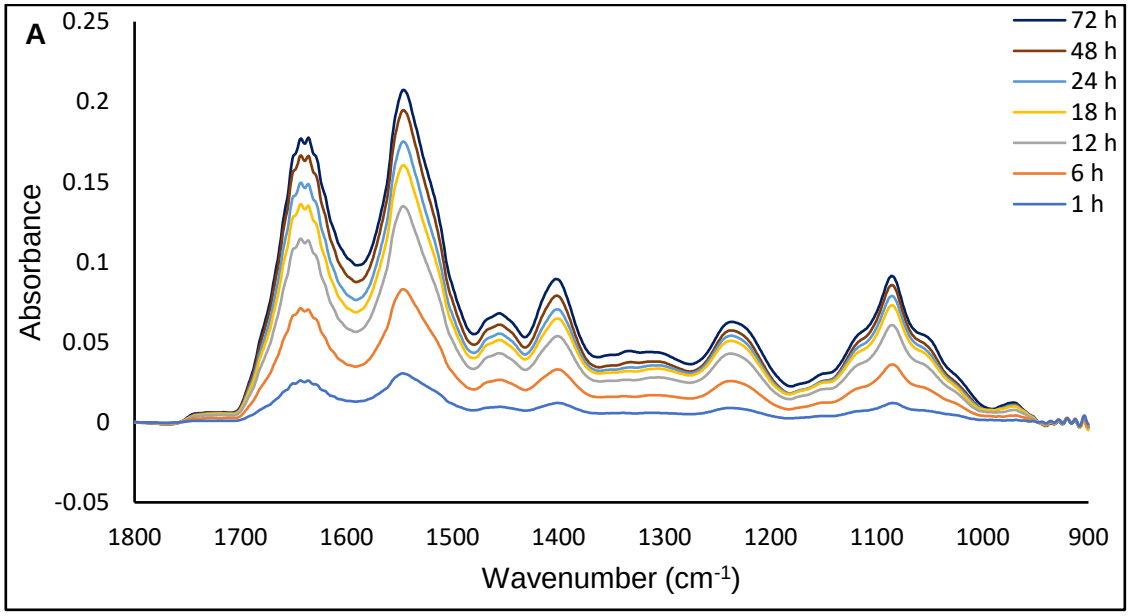

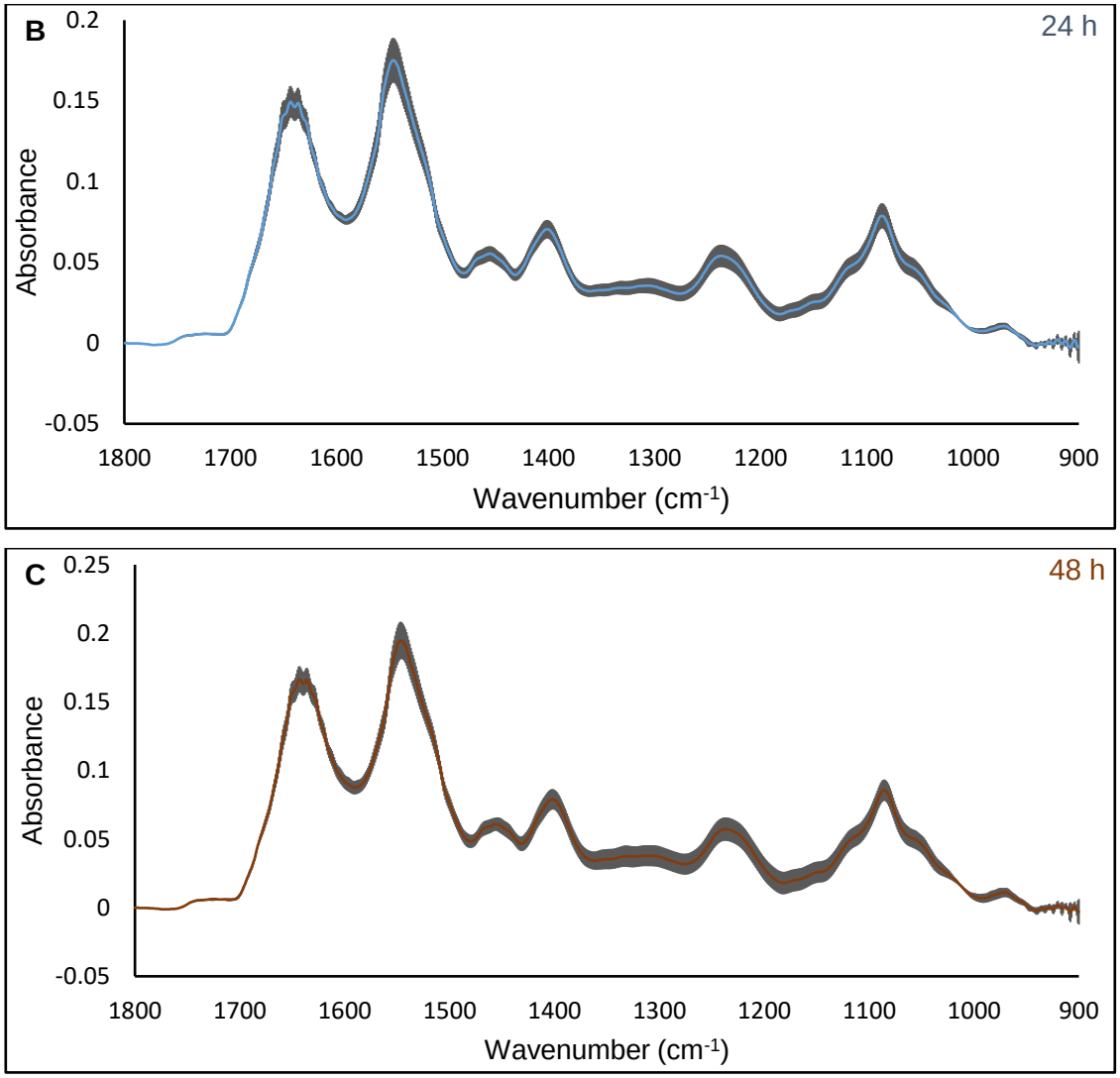

Figure 1: Representative ATR FTIR spectra of MCF7 cells seeded on the ATR element for 72 h (**A**). The spectra are an average of four independent FTIR measurements. A straight line between 1800-950 cm^{-1} was used to baseline the spectra. The error bars of the 24th and 48th h average spectra presented in (**B**) and (**C**), respectively (n=4). The grey colour in (**B**) and (**C**) indicate the standard deviations of the measurements for every wavenumber (cm^{-1}).

In the previous study, we have demonstrated that studying spectral changes of cells at the IC50 (the concentration required to cause 50% reduction in the growth of cells after 24 h) produced the most clear grouping of drugs according to their modes of action.[25] IC50 is also a commonly used concentration in the screening for new drugs and, therefore, it is used as a reference concentration in this study to normalise the possible variations in the performance of the drugs due to differences in the rate of drug uptake and transport. The percentage viability of MCF7 treated with tamoxifen, toremifene and doxorubicin for 24 hours were determined by the 3-(4,5-dimethylthiazol-2-yl)-2,5-diphenyltetrazolium bromide (MTT) assay are shown in (**Figure 2, A-C**) and in **Table 1**.

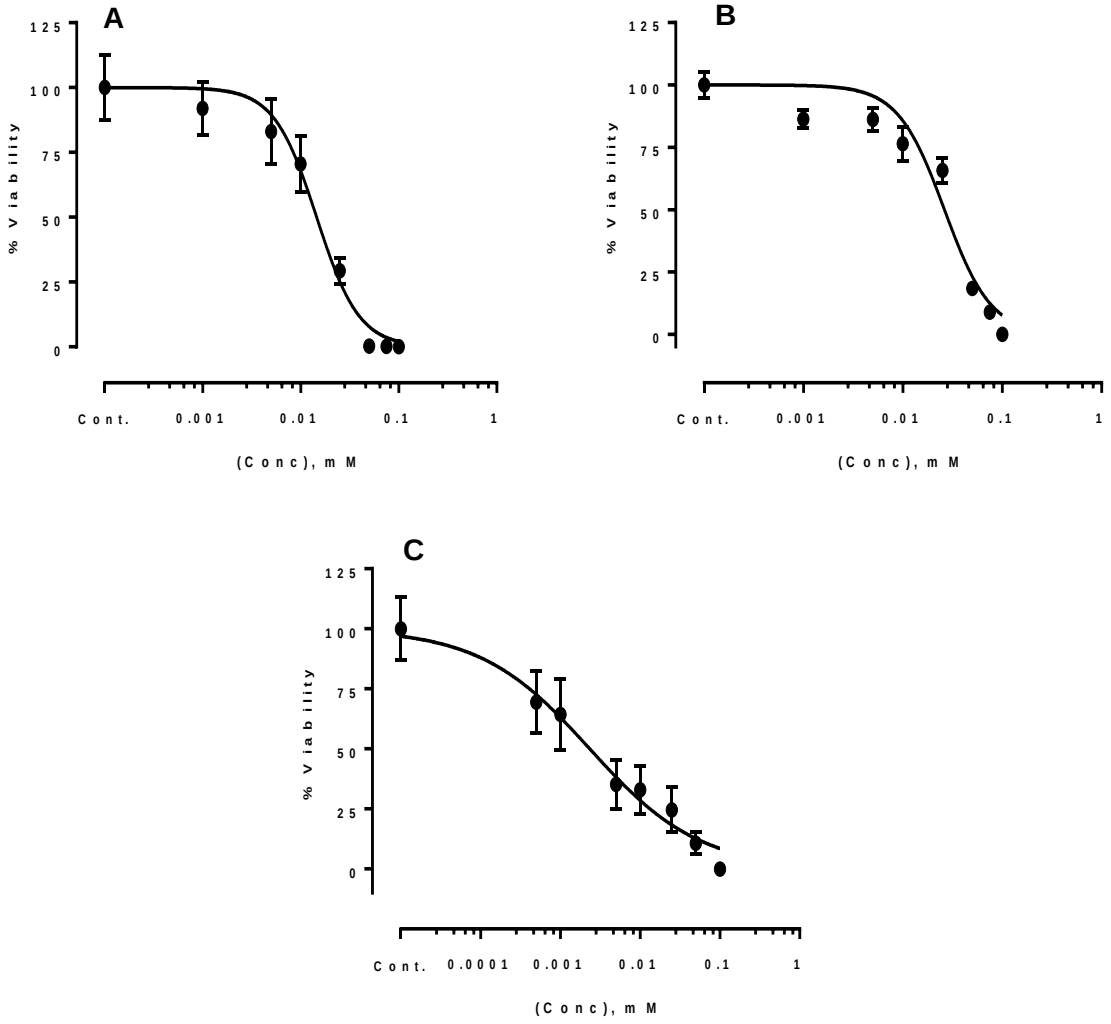

Figure 2: Viability percentage of MCF7 cells seeded in L-15 medium and treated with tamoxifen (**A**), toremifene (**B**), and doxorubicin (**C**) for 24 h. Data are presented as mean ± SD of three independent MTT assays.

Table 1: Summary of the calculated IC50 against MCF7 cells and the mode of actions of drugs used in this study.

Drug	**Mode of Action**	**IC50 (µM)**
Tamoxifen	Selective Oestrogen Receptor Modulator (SERMs) also known as Oestrogen-Dependent Pathway mainly in ER-positive breast cancer (e.g. MCF7)	~14.5
Toremifene	Selective Oestrogen Receptor Modulator (SERMs) also known as Oestrogen-Dependent Pathway mainly in ER-positive breast cancer (e.g. MCF7)	~23.3
Doxorubicin	DNA-Intercalating Agent	~ 2.1

The effect of tamoxifen and toremifene on the oestrogen positive breast cancer (e.g. MCF7) are believed to be mediated through competitive binding to oestrogen receptors (ER) against oestrogen, which is also known as a classical genomic mechanism. Other studies also suggested a non-genomic mechanism that is mediated through the epidermal growth factor receptor (EGFR), which leads to sustained phosphorylation of ERK 1/2 in ER-positive cancer cell lines (MCF-7 and T47D).[28, 29] Doxorubicin is a broad spectrum anthracycline anticancer agent that is very effective in the treatment of many cancer types and widely used in the treatment of breast cancer cells.[30] The *in vitro* effect of doxorubicin on the MCF7 and MDA-MB-231 cells is well-established. For example, some studies have shown multiple mechanisms at the molecular level of the doxorubicin DNA intercalation effects in breast cancer, which eventually leads to the induction of apoptosis and cells death.[31]

The acquired data were pre-processed as previously described.[25] The first spectrum measured immediately after adding the drugs was used as a background, which was ratioed to subsequent spectra to obtain the difference spectra. The difference spectra underline the subtle spectral changes of cells after the introduction of anticancer drugs. Since spectra were collected at 20 min intervals, many time-points can be analysed individually. To maintain the simplicity of the presentation, vector normalised difference spectra acquired at the 2nd, 4th and 6th hours of exposure to drugs have been selectively presented in **(Figure 3, A-C)**. The difference spectra of untreated cells (control) mainly highlights the typical spectrum of cells due to the continual incremental growth of the cell, as previously shown in (**Figure 1**). In comparison to the control, the drug-treated MCF7 cells demonstrated different spectral changes mainly in the 1240-950 cm^{-1} region where absorbance peaks of cellular components such as nucleic acids, phosphorylated compounds and carbohydrates can be identified. Tamoxifen and toremifene, which belongs to the same class of anticancer drugs (i.e. SERMs) prominently show similar spectral changes that are different from the control and the doxorubicin-treated cells. Furthermore, the doxorubicin-treated MCF7 cell spectrum shows a reduction in the absorbance of peaks at 1085 cm^{-1} and 1050 cm^{-1} regions at the 2nd hours of exposure, which become more apparent at the 4th and 6th hours of exposure**,** while amide II bands ~ 1545 cm^{-1} showed no significant changes **(Figure 3, B and C)**. These changes have been previously recognised in PC-3 cells treated with 1.0 µM doxorubicin and in MDA-MB-231 cells treated with IC50 of doxorubicin (~3 µM), which is attributed to the breakage of the phosphates backbone of the DNA because of the intercalation effect of doxorubicin.[24, 25]

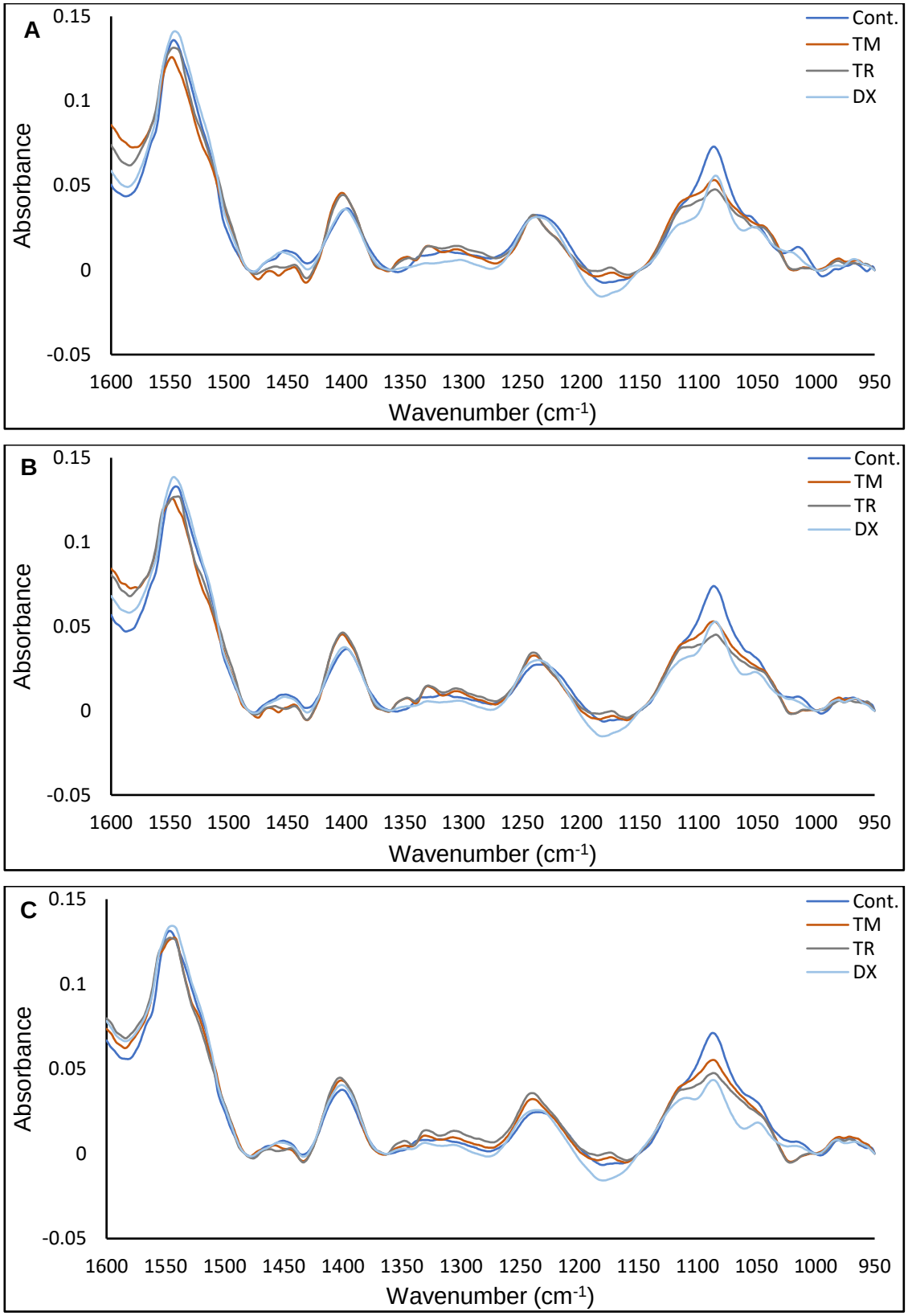

Figure 3: FTIR (vector normalised) difference spectra of live MCF7 cells after exposure to 0.1% DMSO (drug vehicle; control(C)) and IC50 of tamoxifen (TM), toremifene (TR), and doxorubicin (DX) for 2, 4 and 6 h (**A**, **B**, and **C**, respectively). The spectra presented are an average of four repeated measurements for each condition. Refer to (**supplementary Figure S5**) for the average spectra with error bars.

Principal component analysis (PCA) of the difference spectra of control and drug-treated MCF7 cells are shown in **Figure 4**. The score (which highlights the "intensity") and the corresponding loading (which highlights the spectral pattern) plots of first two PCs at 2^{nd}, 4^{th} and 6^{th} hours of live MCF7 cells exposed to the IC50 of tamoxifen, toremifene and doxorubicin are shown in **Figure 4 A-C, respectively**. First, it can be observed that the score plots of PC1 versus PC2 of the 2^{nd}, 4^{th} and 6^{th} hour clearly separated tamoxifen/toremifene treated MCF7 cells from doxorubicin-treated and from untreated cells (control). Most importantly, tamoxifen and toremifene-treated MCF7 cells always clustered relatedly, which again confirmed the remarkable similarity observed from the difference spectra shown in **Figure 3, A-C**. Additionally, the PCA loading plots demonstrated a time-dependent spectral change in which the loadings of PC1 and PC2 in the 2^{nd} hour of exposure is different from that of 6^{th} hour of exposure. In **Figure 4A**, for example, the PC1 of the 2^{nd} hour (accounted for 57.58% of the major variances) mainly separated tamoxifen/toremifene-treated MCF7 cells from doxorubicin-treated cells and control and highlighted spectral changes at 1020, 1087, 1172, 1225, 1410 and 1508 cm^{-1}. The peaks at 1172, and 1508 cm^{-1} overlaps with the spectrum of tamoxifen and toremifene and are possibly indicative of drug accumulations in the cells **(**refer to **Supplementary Figure S6)**. However, other peaks that are notably detected in the same PC1 loadings are not originated from the absorbance of the drugs and accounted for the grouping as well. PC2 score (22.20% of the variances) and loading plots of the 2^{nd} hour exposure highlighted changes at 1200-1240 and 1085 cm^{-1} and mainly separated doxorubicin-treated cells from control as presented in (**Figure 4A)**. These bands are characteristic of the asymmetric (~1237 cm^{-1}) and symmetric phosphodiester vibrations of nucleic acids (~1085 cm^{-1}) and could be an indication of DNA-intercalating mechanism of doxorubicin. The score plot of PC1 versus PC2 for the 4^{th} hour shown in (**Figure 4B)** once again provided a grouping of the drugs in a similar pattern (with an inverted sign) as previously observed in the 2^{nd} hour exposure (**Figure 4A**). The PC1 represented 58.40% of the variances and separated tamoxifen/toremifene-treated MCF7 cells from doxorubicin-treated cells and control and highlighted the same spectral changes as observed in Figure 4A (with an inverted sign). Compared to the 2^{nd} hour of exposure, the contribution of tamoxifen/toremifene accumulations peaks (i.e. bands at 1508 and 1172 cm^{-1}) was weaker. At the 6^{th} hour of exposure, the score plot of PC1 versus PC2 continues to show a clear separation between the drugs with different mode of actions as shown in **Figure 4C**. However, PC1 (49.53% of the variances) mainly in this case separated doxorubicin-treated cells from tamoxifen/toremifene and untreated cells. The PC1 loadings remarkably highlighted spectral changes at 1240-1200 and 1085 cm^{-1} that are associated with DNA-intercalating effects of doxorubicin as previously discussed. PC2 mainly separated tamoxifen/toremifene-treated MCF7 cells and highlighted spectral changes

similar to the PC1 at the 2nd and 4th hour of treatment with a diminished contribution from the 1508 cm^{-1} band.

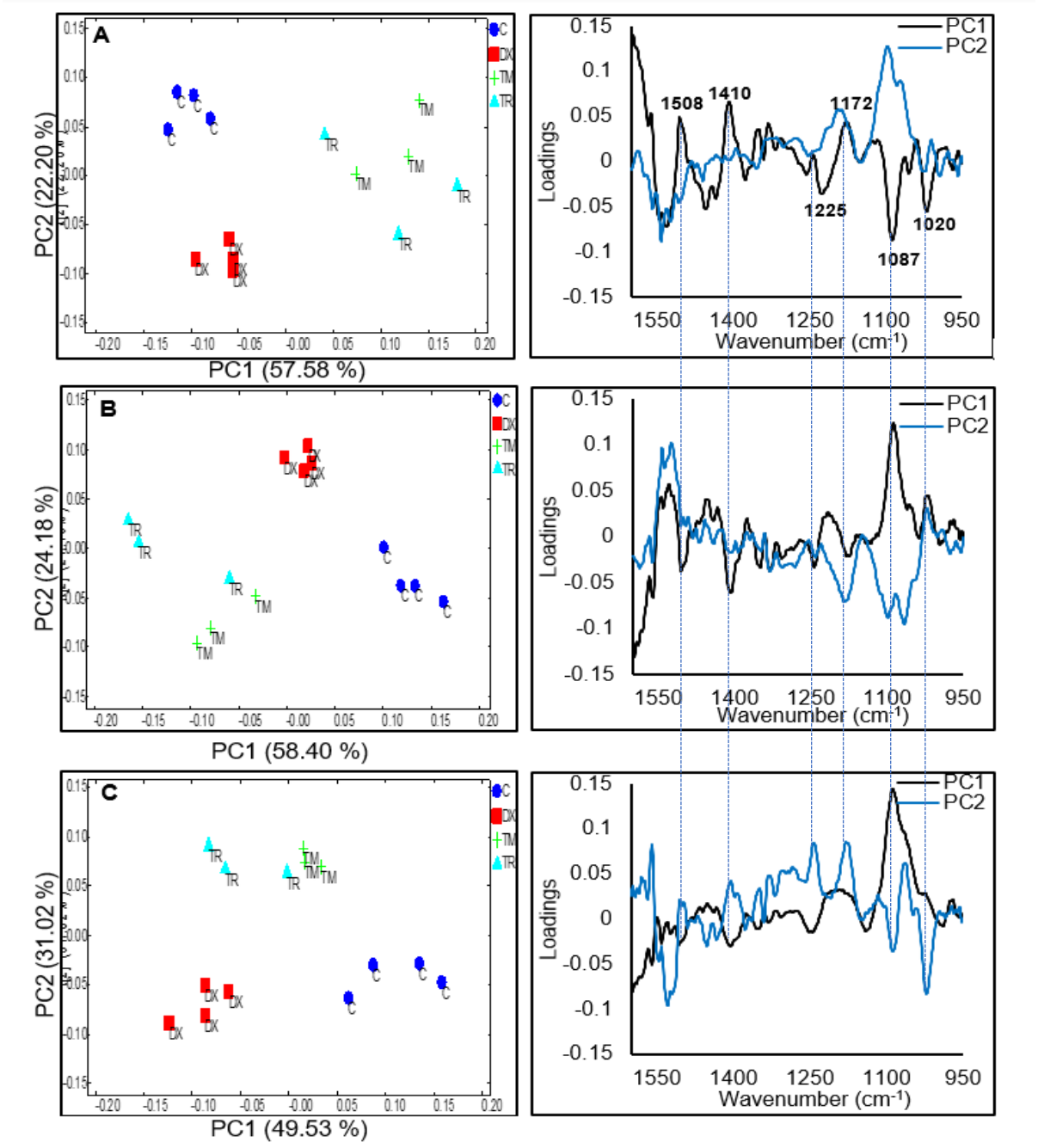

Figure 4: PCA scores and their corresponding loadings of FTIR vector normalised difference spectra of live MCF7 cells after exposure to 0.1% DMSO (Control) and IC50 of tamoxifen (TM), toremifene (TR), and doxorubicin (DX) in the 2nd h (**A**), 4th h (**B**) and 6th h (**C**). Vertical lines were added to the loading plots to aid in the comparison between the different hours of treatment.

Importantly, the PCA loadings of the live MCF7 cells exposed to drugs at different time points grouped drugs according to their modes of actions and remarkably highlighted spectral changes in the 1250-950 cm^{-1} region. Absorbance peaks in this particular region are indicative

of changes in the asymmetric PO_2^- of nucleic acids, phosphorylated proteins (~1237 cm^{-1}), C-O of carbohydrates and proteins side chains (~1150 cm^{-1}), symmetric PO_2^- of nucleic acids and PO_4^{2-} phosphorylated proteins, C-O-C and C-O-P of polysaccharides (~1080 cm^{-1}), C-O of carbohydrates (~1050-1036 cm^{-1}) and PO_4^{2-} of phosphorylated proteins and nucleic acids (~990-970 cm^{-1}). It is worth mentioning that spectral changes in the 1250-950 cm^{-1} region have been previously demonstrated in MDA-MB-231 cells exposed to the IC50 of tamoxifen/toremifene, imatinib and doxorubicin. In a similar approach to the one employed in this study, PCA of the 2nd, 4th and 6th hours grouped drugs with a similar mode of actions in the same cluster while drugs with different modes of actions were clustered separately.[25] Further investigation, as we shall discuss later, will underline if the spectral changes due to the exposure to the same drug will be similar in different cell lines with different properties.

Comparison Between MCF7 and MDA-MB-231 Cells

The response of MCF7 and MDA-MB-231 cells treated with the IC50 of tamoxifen, toremifene and doxorubicin have been investigated to determine whether the different modes of action of the same drug in different cell lines can be detected using the live cell FTIR approach. The results from the pairwise PCA (SERM drugs-treated *versus* control) for the MCF7 and MDA-MB-231 cells at a specific length of time of exposure are shown in Figure 5 and 7. In all pairwise PCA, PC1 represented more than 70% of the variances and is the only PC that provides a clear separation between the drug-treated cells and the control cells. . The pairwise PCA of the spectral response of MCF7 cells and MDA-MB-231 has shown a clear separation after the 2nd hour of exposure to the IC50 tamoxifen/toremifene (**Figure 5, A-C**). Although similar spectral changes were detected in the 1600-1400 cm^{-1} region, remarkably difference can be observed in the 1400-900 cm^{-1} region suggesting these drugs has different modes of actions in the MCF7 and MDA-MB-231 cells. Tamoxifen/toremifene are known SERMs, and their classical modes of actions in ER-positive cancer cells (i.e. MCF7) are mainly mediated through their competition with oestrogen for binding to the oestrogen receptor (ER), which eventually lead to the induction of cell death. The MDA-MB-231 cells, also known as triple negative cells, lack the expression of ER, progesterone receptor (PR) and human epidermal growth factor receptor 2 (HER2). The cytotoxicity of tamoxifen against MDA-MB-231 is well-established and demonstrated to be mediated through the inhibition of protein phosphatase 2A (CIP2A) and phospho-Akt (p-Akt).[27, 32] Moreover, tamoxifen induces cells death in both ER-positive (MCF7) and ER-negative (MDA-MB-231) cells by rapid mitochondrial death program that involves an increase in the production of reactive oxygen species (ROS), the release of cytochrome c and decrease in the mitochondrial membrane potential.[28, 33] The dissimilarity in the response of MCF7 and MDA-MB-231 cells to tamoxifen/toremifene at the same cytotoxicity level (i.e. IC50) reflected the different modes of actions of tested drugs on these two cell lines.

Likewise, the pairwise PCA of the response of MCF7 cells and MDA-MB-231 after the 2nd hour of exposure to the IC50 of doxorubicin are shown in (**Figure 6, A-C**). The PC1 loadings of MDA-MB-231 cells (black spectrum) and MCF7 cells (red spectrum), to some extent, show similarity in the 1150-950 cm^{-1} region with a significant decrease in absorbance of the band at 1087 cm^{-1}. This band is mainly associated with the symmetric phosphodiester vibrations of nucleic acids (~1085 cm^{-1}), which is expected from the DNA-intercalating effects of doxorubicin in these two cell lines. The differences in response observed in the 1250-1150 cm^{-1} possibly originated from other cellular metabolites that are originated from upstream or downstream signalling cascades due to the DNA-intercalations. As previously mentioned, different mechanisms have been demonstrated to explain the role of doxorubicin in the DNA-intercalation such as the generation of free radicals, inhibition of topoisomerase II enzyme and the interference of helicase activity and DNA unwinding.[31, 34] Doxorubicin has also been demonstrated to induce transcriptional changes with many variations between cell types.[35, 36] The pairwise analysis of the 4th and 6th hr of MCF7 and MDA-MB-231 cells in response to each of the drugs demonstrated similar spectral changes (PCs loadings) to the 2nd hour and the results are presented in (**see supplementary, Figures S7 and S8**).

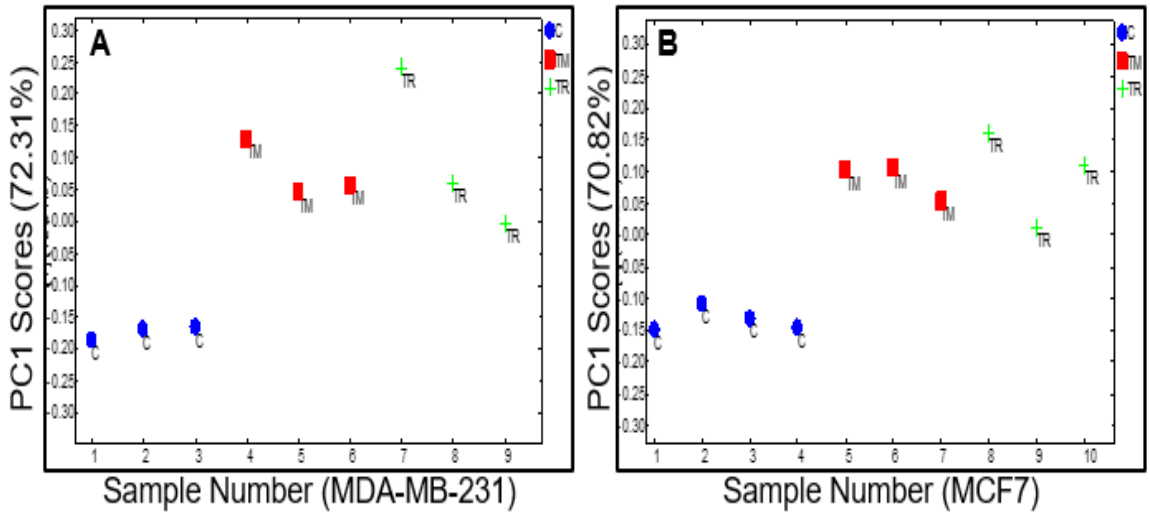

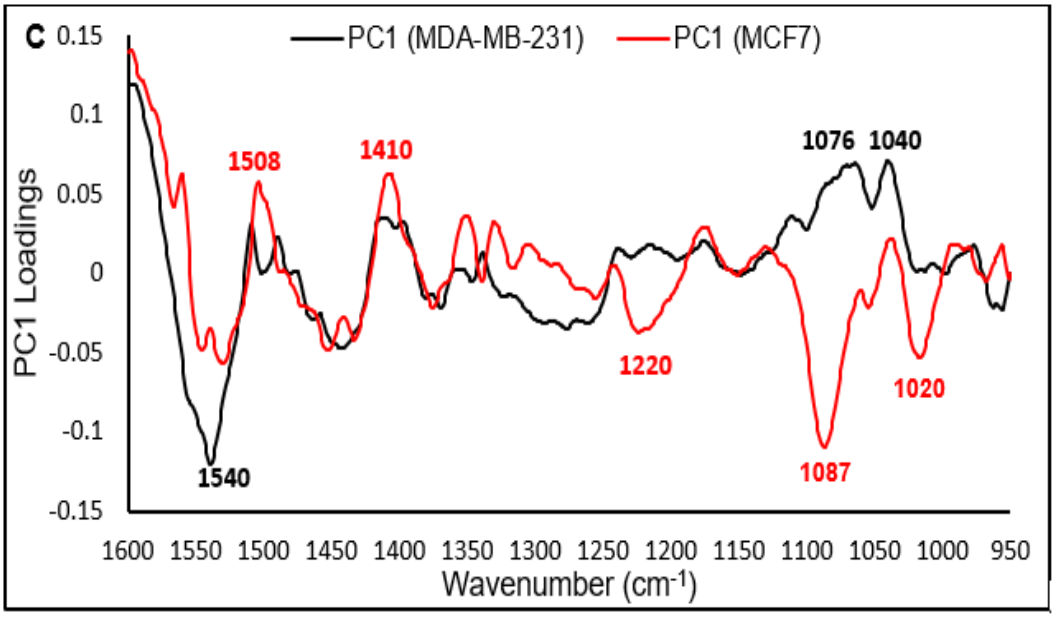

Figure 5: (**A**) shows the pairwise PC1 scores of MDA-MB-231 cells for control (1-3) versus tamoxifen (4-6) and toremifene (7-9). (**B**) represents the pairwise PC1 score of MCF7 cells for control (1-4) versus tamoxifen (5-7) and toremifene (8-10). (**C**) demonstrates the corresponding PC1 loadings of MDA-MB-231 cells (black spectrum) and MCF7 (red spectrum) after the 2nd h of exposure to the IC50 of tamoxifen/toremifene.

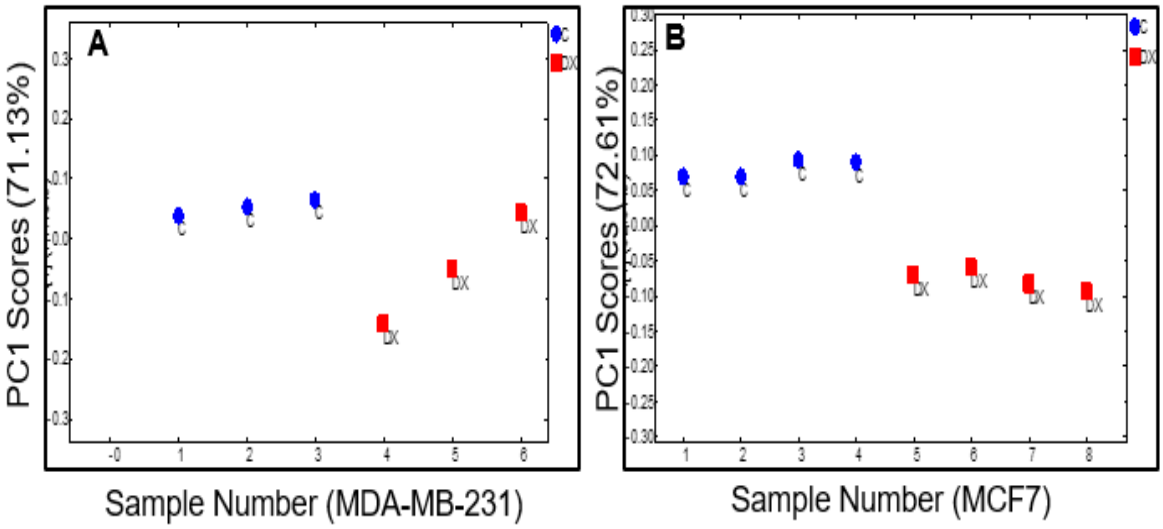

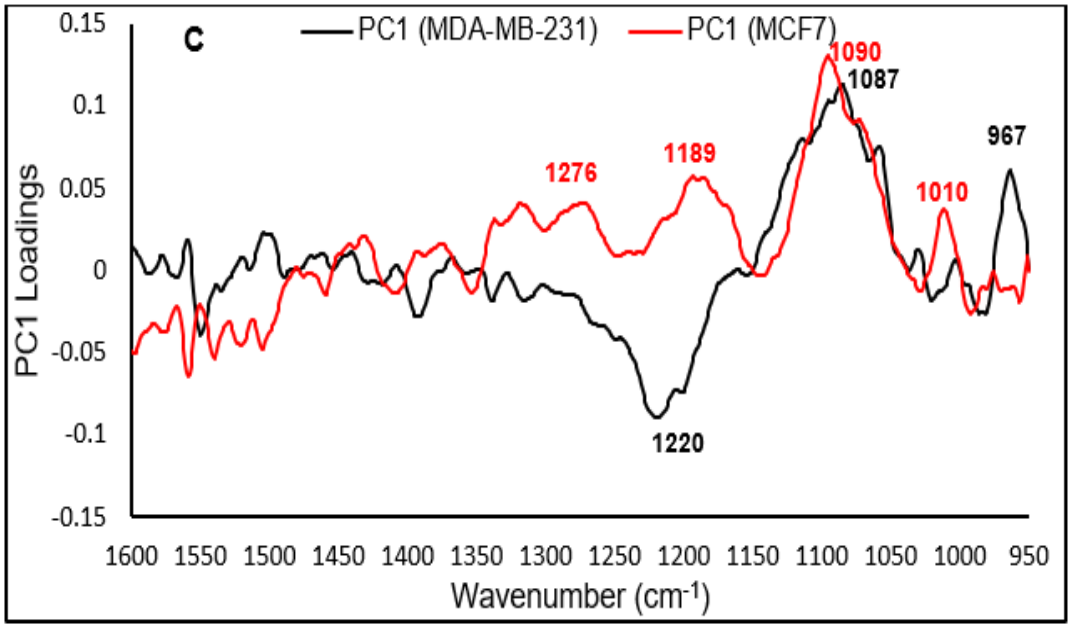

Figure 6: (**A**) shows the pairwise PC1 scores of MDA-MB-231 cells for control (1-3) versus doxorubicin (4-6). (**B**) represents the pairwise PC1 scores of MCF7 cells for control (1-4) versus doxorubicin (5-8). (**C**) demonstrates the corresponding PC1 loadings of MDA-MB-231 cells (black spectrum) and MCF7 (red spectrum) after the 2nd hour of exposure to the IC50 of doxorubicin.

Conclusion

In this study, live-cell FTIR spectroscopy has been demonstrated as a powerful technique to distinguish the modes of actions between different drugs on the same cell line and the different response to the same drug fromcell lines of different characteristics. The difference spectra of MCF7 cells treated in IC50 of tamoxifen and toremifene, which belong to the same anticancer class (SERMs), show remarkable similar spectral changes. However, doxorubicin treated MCF7 cells presented spectral changes that are different from cells treated in tamoxifen/toremifene. These changes mainly occurred in the spectral regions at 1085, and 1200-1240 cm^{-1}, which could be associated with the DNA-intercalation effects of doxorubicin. The pairwise PCA confirms that MCF7 cells responded differently to the SERMs in comparison to the triple negative MDA-MB-231 cells when treated in the SERMs, which is another evidence of the cell line-dependent modes of actions of these drugs. These results are in good agreement with several studies, which have shown that SERMs can induce their cytotoxic effect either in an oestrogen-dependent pathway (for oestrogen-positive cells such as MCF7) or oestrogen-independent pathway (for oestrogen-negative cells such as MDA-MB-231).

Furthermore, the pairwise PCA of doxorubicin-treated cells demonstrated a remarkable similarity between the two cell lines in the 1150-950 cm^{-1} regions, highlighting the DNA

intercalating effect of the drug, but some variations were observed at 1200-1250 cm^{-1}. This indicates that the response of different breast cancer cells to doxorubicin is not entirely the same, and several types of breast cancer cells should be tested in the future. In summary, live-cell FTIR method holds a promising potential in distinguishing drugs according to their modes of action. A further collection of live-cell data will help in designing a discrimination model to predict the modes of action of anticancer molecules and eventually can be employed in pre-clinical screening for novel anticancer drugs.

Experimental Section

Multi-bounce ATR-FTIR accessory

A 10-reflection (10 internal reflections on the sample side) ATR accessory trough plate (HATR, Pike technologies) controlled at 37℃ with a 45° ZnS ATR element (80 mm X 10 mm X 4 mm, Crystan Ltd., UK) was used. A schematic is shown in Figure 7. The effective path length obtained in the living cells produced from this accessory is approximately 20-30 µm, with a depth of penetration ($\mathbf{d_p}$) nearly 2-3 µm. The trough plate has a measurement surface of about 500 mm^2, where live cells adhere and continuously measured.

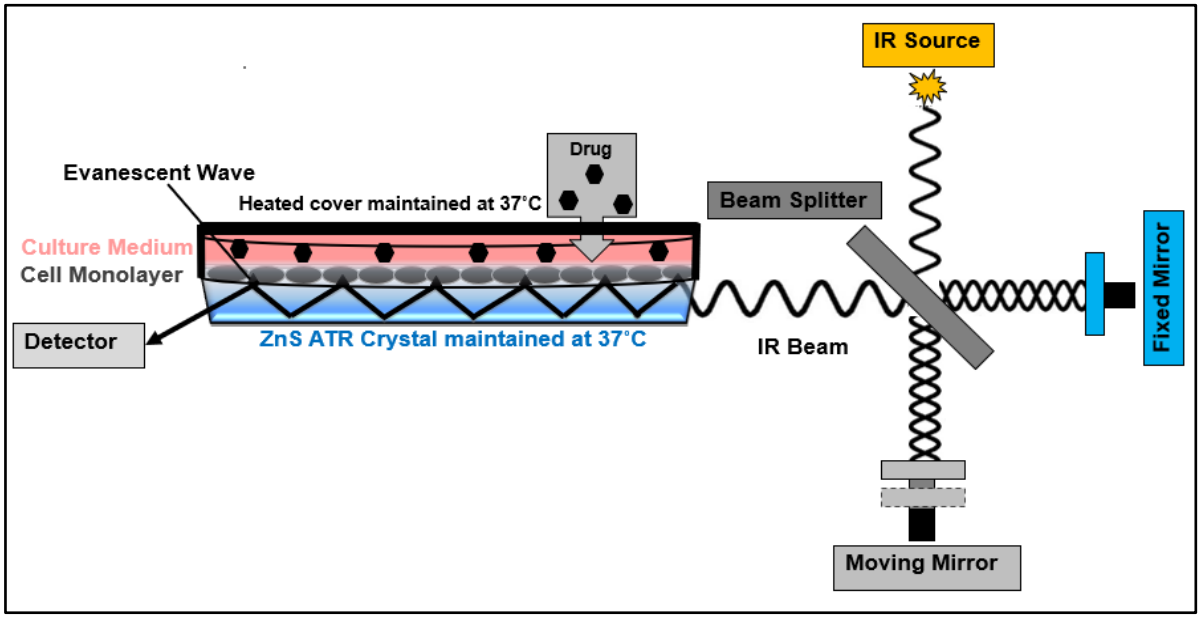

Figure 7: A schematic describing the ATR element and the cell culture set up for the live cells FTIR measurement. An IR beam from the interferometer is shone on the live cells intimately adhered to ATR surface and undergoes internal reflections. The generated evanescent wave penetrates (~2-3 µm) and absorbed by the sample (cells), which then converted to an ATR absorbance spectrum by Fourier transform.

Live cell preparation

MCF7 cells were maintained in T25 cell culture flasks using DMEM high glucose medium with 10% FBS, 1% MEM NEAA, 2 mM L-glutamine, 100 U/mL penicillin and 100 U/mL streptomycin and incubated in a 5% CO_2 and 37°C incubator. The cells were trypsinised and harvested when they reached ~80% confluence and then centrifuged into a pellet. The pellet was then re-suspended in L-15 medium, supplemented with 10% FBS, 1% MEM NEAA, 2 mM L-glutamine, 100 U/mL penicillin and 100 µg/mL streptomycin, to reach a cell density of ~ 5.0 x 10^5 cells/mL and total of 2.0 mL of suspension (i.e. ~ 1.0 X 10^6 cells). The cell suspension was directly seeded onto the multi-reflection trough plate controlled at 37 °C and sealed with a heated glass cover lid at 37 °C, to control the temperature in the measurement chamber. After 24 hours of incubation, the high seeding density ensured that cells are attached to the measurement surface as a monolayer with high (~90%) confluence. A reflective optical microscope with a 10x objective (L2003 microscope fitted with a digital camera) was used to confirm the confluence and attachment of cells to the measurement surface (**see supplementary Figure S1**).

Determination of cell viability

The viability of cells was determined using the standard MTT (3-(4,5- dimethylthiazol-2-yl)-2,5-diphenyltetrazolium bromide) assay.[37] In brief, suspension of MCF7 cells (2 x 10^4 cells per well) in L-15 medium was seeded in a 96-well plate and allowed to grow for 24 hours at 37 °C to reach a comparable confluence (~90%) to the ATR-FTIR experiment. The medium was then replaced with the L-15 medium, which contains different concentrations of tamoxifen, toremifene (dissolve in DMSO) and doxorubicin (dissolved in water) and incubated at 37 °C for 24 hours. In all treatments, the final concentration of DMSO was maintained at 0.1%. Afterwards, the supernatant of each well was removed, washed once with PBS medium and replaced with 100 µL (0.5 mg/mL) of MTT in L-15 medium. The 96-well plate was incubated for 3 hours before discarding the MTT solution. In the last step, 100 µL per well of DMSO was added to dissolve the resulted formazan product and the absorbance was measured at 570 nm, with the reference at 630 nm, in a Spectra MAX 190 multi-well plate reader. The relative cell viability percentage was calculated by comparing the absorbance of treated cells with control, where 0.1% DMSO in L-15 medium was applied instead of the drug solution. GraphPad Prism® was used to calculate the IC50 and data presented as mean ± SD.

FTIR measurement of samples

An FTIR spectrometer (Frontier, Perkin Elmer Ltd., UK) fitted with a room temperature deuterated triglycine sulfate (DTGS) detector. After seeding the cells in the ATR trough plate for 24 hours, the cells attached to the ZnS ATR element were exposed to the IC50 of tamoxifen, toremifene and doxorubicin by adding appropriate amounts of 50 mM stock solution in the L-15 medium and maintain a total of 0.1% DMSO. Cell spectra were measured by averaging ~237 scans (scanning time of 11 minutes) and were acquired every 20 minutes so that three spectra were collected hourly (i.e. 144 spectra were collected within the 48 hour period). The IR spectrum of cells measured in spectral region of 2000 to 900 cm^{-1} with a spectral resolution of 8 cm^{-1} and 0.2 cm/s mirror speed. A strong Norton-Beer apodization function and self-phase correction selected for the interferogram process. Spectrum 10 software (Perkin Elmer Ltd., UK) used for the data processing, including baseline and the water vapour correction. Spectra of cells were continuously monitored from the moment after seeding the cells on the ATR element for 24 hours. For control, DMSO was added to the medium on the ATR trough to reach a concentration of 0.1% and measured for another 24 hours. A spectrum of L-15 medium was used as a background to obtain the full spectra of cells with the water vapour subtracted. For difference spectra, the first spectrum of cells immediately after the addition of drugs was used as a background to highlight the changes in live cells (**see supplementary Figure S2**). All experiments were repeated at least three times.

Principal Component Analysis (PCA)

PCA was carried out using PyChem Software (http://pychem.sourceforge.net/).[38] This analysis was applied to reduce the dimension of the spectroscopic data. Correlation matrix and Nonlinear Iterative Partial Least Squares (NIPALS) were selected for the PCA analysis. The data pre-processing performed as previously described in [25]. Briefly, the spectral wavenumber range was truncated to 1800-900 cm^{-1}, and then an interactive baseline correction using the Spectrum 10 software (Perkin Elmer) was performed based on the minima absorbance at 2000, 1800, 1757, 1480, 1000 and 950 cm^{-1}. Vector normalisation was calculated in Microsoft ®Excel 10, in which spectra were divided by the square root of the sum of the mean intensities squared. PCA was applied to analyse spectra extracted from different time points after the addition of drugs. The analysis was focused on the first two principle components (i.e. PC1 and PC2) as they accounted for more than 85% of the variances (**Supplementary, Figure S3**). The amide I region (~1640 cm^{-1}) was excluded in the PCA as the water peak at this region exceeded 1, which indicates that the detector will not operate in a linear response at this band (**Supplementary, Figure S4**).[23, 39]

AUTHOR INFORMATION

Corresponding Author

*Please direct all correspondence to ka_lung.chan@kcl.ac.uk

Author Contributions

KLAC and KMR conceived the idea, AA carried out all experimental works, processed the data and written the draft. KLAC and AA interpreted the data. All authors proof-read the draft.

Competing Interests

The authors declare no competing financial interest.

ACKNOWLEDGEMENTS

KLAC thanks EPSRC (grant number EP/L013045/1) for support. Ali Atharawi thanks Prince Sattam Bin Abdulaziz University (Saudi Arabia) for his PhD sponsorship.

Supplementary Materials

The following materials are available online:

Figure S1: Visible image of MCF7 cells on the ZnS ATR crystal

Figure S2: Spectra of cell after various treatments

Figure S3: Cumulative variance versus number of principle component plot

Figure S4: ATR FTIR spectrum of water

Figure S5: Difference spectra of MCF7 cells after various treatments

Figure S6: Spectra of drugs in solution

Figure S7: Pairwise (drug treated and control) PCA analysis at 4 h after treatment

Figure S8: Pairwise (drug treated and control) PCA analysis at 6 h after treatment

ABBREVIATIONS

ATR	attenuated total reflection
DNA	deoxyribonucleic acid
EGFR	epidermal growth factor receptor
ER	oestrogen receptors
FTIR	Fourier transform infrared
HER2	human epidermal growth factor receptor 2
MTT	3-(4,5-dimethylthiazol-2-yl)-2,5-diphenyltetrazolium bromide
PC1	principal component 1
PC2	principal component 2
PCA	principal component analysis
PR	progesterone receptor
ROS	reactive oxygen species
SERMs	selective estrogen receptor modulators
SNR	signal-to-noise ratio

References

1. Hambley, T. W., Is Anticancer Drug Development Heading in the Right Direction? *Cancer Research* **2009,** *69* (4), 1259-1261.

2. Hait, W. N., Anticancer drug development: the grand challenges. *Nat. Rev. Drug Discov.* **2010,** *9* (4), 253-254.

3. Hutchinson, L.; Kirk, R., High drug attrition rates-where are we going wrong? *Nat. Rev. Clin. Oncol.* **2011,** *8* (4), 189-190.

4. Moreno, L.; Pearson, A. D. J., How can attrition rates be reduced in cancer drug discovery? *Expert Opinion on Drug Discovery* **2013,** *8* (4), 363-368.

5. Wishart, D. S., Applications of metabolomics in drug discovery and development. *Drugs in R&D* **2008,** *9* (5), 307-322.

6. Mikami, T.; Aoki, M.; Kimura, T., The application of mass spectrometry to proteomics and metabolomics in biomarker discovery and drug development. *Current Molecular Pharmacology* **2012,** *5* (2), 301-16.

7. Jamieson, L. E.; Byrne, H. J., Vibrational spectroscopy as a tool for studying drug-cell interaction: Could high throughput vibrational spectroscopic screening improve drug development? *Vibrational Spectroscopy* **2017,** *91*, 16-30.

8. Mignolet, A.; Derenne, A.; Smolina, M.; Wood, B. R.; Goormaghtigh, E., FTIR spectral signature of anticancer drugs. Can drug mode of action be identified? *Biochimica et Biophysica Acta-Proteins and Proteomics* **2016,** *1864* (1), 85-101.

9. Hughes, C.; Clemens, G.; Baker, M. J., Preclinical screening of anticancer drugs using infrared (IR) microspectroscopy. *Trends in Biotechnology* **2015,** *33* (8), 429-430.

10. Zwielly, A.; Gopas, J.; Brkic, G.; Mordechai, S., Discrimination between drug-resistant and non-resistant human melanoma cell lines by FTIR spectroscopy. *Analyst* **2009,** *134* (2), 294-300.

11. Rutter, A. V.; Siddique, M. R.; Filik, J.; Sandt, C.; Dumas, P.; Cinque, G.; Sockalingum, G. D.; Yang, Y.; Sule-Suso, J., Study of Gemcitabine-Sensitive/Resistant Cancer Cells by Cell Cloning and Synchrotron FTIR Microspectroscopy. *Cytometry Part A* **2014,** *85A* (8), 688-697.

12. Derenne, A.; Gasper, R.; Goormaghtigh, E., The FTIR spectrum of prostate cancer cells allows the classification of anticancer drugs according to their mode of action. *Analyst* **2011,** *136* (6), 1134-1141.

13. Berger, G.; Gasper, R.; Lamoral-Theys, D.; Wellner, A.; Gelbcke, M.; Gust, R.; Neve, J.; Kiss, R.; Goormaghtigh, E.; Dufrasne, F., Fourier Transform Infrared (FTIR) spectroscopy to monitor the cellular impact of newly synthesized platinum derivatives. *International Journal of Oncology* **2010,** *37* (3), 679-686.

14. Gasper, R.; Dewelle, J.; Kiss, R.; Mijatovic, T.; Goormaghtigh, E., IR spectroscopy as a new tool for evidencing antitumor drug signatures. *Biochim. Biophys. Acta-Biomembr.* **2009,** *1788* (6), 1263-1270.

15. Gasper, R.; Mijatovic, T.; Benard, A.; Derenne, A.; Kiss, R.; Goormaghtigh, E., FTIR spectral signature of the effect of cardiotonic steroids with antitumoral properties on a prostate cancer cell line. *Biochimica et Biophysica Acta-Molecular Basis of Disease* **2010,** *1802* (11), 1087-1094.

16. Derenne, A.; Verdonck, M.; Goormaghtigh, E., The effect of anticancer drugs on seven cell lines monitored by FTIR spectroscopy. *Analyst* **2012,** *137* (14), 3255-3264.

17. Flower, K. R.; Khalifa, I.; Bassan, P.; Demoulin, D.; Jackson, E.; Lockyer, N. P.; McGown, A. T.; Miles, P.; Vaccari, L.; Gardner, P., Synchrotron FTIR analysis of drug treated ovarian A2780 cells: an ability to differentiate cell response to different drugs? *Analyst* **2011,** *136* (3), 498-507.

18. Hobro, A. J.; Smith, N. I., An evaluation of fixation methods: Spatial and compositional cellular changes observed by Raman imaging. *Vibrational Spectroscopy* **2017,** *91*, 31-45.

19. Whelan, D. R.; Bambery, K. R.; Heraud, P.; Tobin, M. J.; Diem, M.; McNaughton, D.; Wood, B. R., Monitoring the reversible B to A-like transition of DNA in eukaryotic cells using Fourier transform infrared spectroscopy. *Nucleic Acids Research* **2011,** *39* (13), 5439-5448.

20. Wood, B. R., The importance of hydration and DNA conformation in interpreting infrared spectra of cells and tissues. *Chemical Society Reviews* **2016,** *45* (7), 1980-1998.

21. Doherty, J.; Zhang, Z.; Wehbe, K.; Cinque, G.; Gardner, P.; Denbigh, J., Increased optical pathlength through aqueous media for the infrared microanalysis of live cells. *Analytical and Bioanalytical Chemistry* **2018,** *410* (23), 5779-5789.

22. Kuimova, M. K.; Chan, K. A.; Kazarian, S. G., Chemical imaging of live cancer cells in the natural aqueous environment. *Applied spectroscopy* **2009,** *63* (2), 164-171.

23. Chan, K. L. A.; Fale, P. L., Label-free in situ quantification of drug in living cells at micromolar levels using infrared spectroscopy. *Analytical Chemistry* **2014,** *86* (23), 11673-11679.

24. Fale, P. L.; Altharawi, A.; Chan, K. L. A., In situ Fourier transform infrared analysis of live cells' response to doxorubicin. *Biochimica et Biophysica Acta (BBA)-Molecular Cell Research* **2015,** *1853* (10 Part A), 2640-2648.

25. Altharawi, A.; Rahman, K. M.; Chan, K. L. A., Towards identifying the mode of action of drugs using live-cell FTIR spectroscopy. *Analyst* **2019,** *144* (8), 2725-2735.

26. Shoemaker, R. H., The NCI60 human tumour cell line anticancer drug screen. *Nat. Rev. Cancer* **2006,** *6* (10), 813-823.

27. Liu, C. Y.; Hung, M. H.; Wang, D. S.; Chu, P. Y.; Su, J. C.; Teng, T. H.; Huang, C. T.; Chao, T. T.; Wang, C. Y.; Shiau, C. W.; Tseng, L. M.; Chen, K. F., Tamoxifen induces apoptosis through cancerous inhibitor of protein phosphatase 2A-dependent phospho-Akt inactivation in estrogen receptor-negative human breast cancer cells. *Breast Cancer Research* **2014,** *16* (5), 431-439.

28. Zheng, A.; Kallio, A.; Harkonen, P., Tamoxifen-induced rapid death of MCF-7 breast cancer cells is mediated via extracellulary signal-regulated kinase signaling and can be abrogated by estrogen. *Endocrinology* **2007,** *148* (8), 3931-3931.

29. Bjornstrom, L.; Sjoberg, M., Mechanisms of estrogen receptor signaling: Convergence of genomic and nongenomic actions on target genes. *Molecular Endocrinology* **2005,** *19* (4), 833-842.

30. Sinha, B. K.; Mimnaugh, E. G.; Rajagopalan, S.; Myers, C. E., Adriamycin activation and oxygen free-radical formation in human-breast tumor-cells - protective role of glutathione-peroxidase in adriamycin resistance. *Cancer Research* **1989,** *49* (14), 3844-3848.

31. Pilco-Ferreto, N.; Calaf, G. M., Influence of doxorubicin on apoptosis and oxidative stress in breast cancer cell lines. *International Journal of Oncology* **2016,** *49* (2), 753-762.

32. Manna, S.; Holz, M. K., Tamoxifen action in ER-negative breast cancer. *Signal Transduction Insights* **2016,** *5* (1), 1-7.

33. Kallio, A.; Zheng, A.; Dahllund, J.; Heiskanen, K. M.; Harkonen, P., Role of mitochondria in tamoxifen-induced rapid death of MCF-7 breast cancer cells. *Apoptosis* **2005,** *10* (6), 1395-1410.

34. Yang, F.; Teves, S. S.; Kemp, C. J.; Henikoff, S., Doxorubicin, DNA torsion, and chromatin dynamics. *Biochimica et Biophysica Acta (BBA)-Reviews on Cancer* **2014,** *1845* (1), 84-89.

35. Bar-On, O.; Shapira, M.; Hershko, D. D., Differential effects of doxorubicin treatment on cell cycle arrest and Skp2 expression in breast cancer cells. *Anti-Cancer Drugs* **2007,** *18* (10), 1113-1121.

36. Taymaz-Nikerel, H.; Karabekmez, M. E.; Eraslan, S.; Kırdar, B., Doxorubicin induces an extensive transcriptional and metabolic rewiring in yeast cells. *Scientific Reports* **2018,** *8* (1), 13672.

37. Mosmann, T., Rapid colorimetric assay for cellular growth and survival: application to proliferation and cytotoxicity assays. *Journal of immunological methods* **1983,** *65* (1-2), 55-63.

38. Jarvis, R. M.; Broadhurst, D.; Johnson, H.; O'boyle, N. M.; Goodacre, R., PYCHEM: a multivariate analysis package for python. *Bioinformatics* **2006,** *22* (20), 2565-2566.

39. Chan, K. L. A.; Fale, P. L., Label-free optical imaging of live cells. In *Biophotonics for Medical Applications*, Elsevier: 2015; pp 215-241.

Table of contents graphic